12-3-2017

Hyperhomocysteinemia-Induced Gene Expression Changes in the Cell Types of the Brain

Erica M. Weekman
University of Kentucky, emweek2@uky.edu

Abigail E. Woolums
University of Kentucky, abigail.woolums@uky.edu

Tiffany L. Sudduth
University of Kentucky, tlsudd2@uky.edu

Donna M. Wilcock
University of Kentucky, donna.wilcock@uky.edu

Hyperhomocysteinemia-Induced Gene Expression Changes in the Cell Types of the Brain

Notes/Citation Information
Published in *ASN Neuro*, v. 9, issue 6, p. 1-11.

Digital Object Identifier (DOI)
https://doi.org/10.1177/1759091417742296

American Society for Neurochemistry

Original Paper

ASN Neuro
November-December 2017: 1–11

DOI: 10.1177/1759091417742296
journals.sagepub.com/home/asn
SAGE

Hyperhomocysteinemia-Induced Gene Expression Changes in the Cell Types of the Brain

Erica M. Weekman[1,2,*], Abigail E. Woolums[1,*], Tiffany L. Sudduth[1], and Donna M. Wilcock[1,2]

Abstract

High plasma levels of homocysteine, termed hyperhomocysteinemia, are a risk factor for vascular cognitive impairment and dementia, which is the second leading cause of dementia. While hyperhomocysteinemia induces microhemorrhages and cognitive decline in mice, the specific effect of hyperhomocysteinemia on each cell type remains unknown. We took separate cultures of astrocytes, microglia, endothelial cells, and neuronal cells and treated each with moderate levels of homocysteine for 24, 48, 72, and 96 hr. We then determined the gene expression changes for cell-specific markers and neuroinflammatory markers including the matrix metalloproteinase 9 system. Astrocytes had decreased levels of several astrocytic end feet genes, such as aquaporin 4 and an adenosine triphosphate (ATP)-sensitive inward rectifier potassium channel at 72 hr, as well as an increase in matrix metalloproteinase 9 at 48 hr. Gene changes in microglia indicated a peak in proinflammatory markers at 48 hr followed by a peak in the anti-inflammatory marker, interleukin 1 receptor antagonist, at 72 hr. Endothelial cells had reduced occludin expression at 72 hr, while kinases and phosphatases known to alter tau phosphorylation states were increased in neuronal cells. This suggests that hyperhomocysteinemia induces early proinflammatory changes in microglia and astrocytic changes relevant to their interaction with the vasculature. Overall, the data show how hyperhomocysteinemia could impact Alzheimer's disease and vascular cognitive impairment and dementia.

Keywords

hyperhomocysteinemia, matrix metalloproteinase, neuroinflammation, vascular cognitive impairment and dementia

Received August 30, 2017; Received revised September 24, 2017; Accepted for publication September 26, 2017

Introduction

Homocysteine is a nonprotein forming amino acid involved in the production of both methionine and cysteine. Mutations in the methylenetetrahydrofolate reductase or cystathionine beta synthase (CBS) genes or low levels of vitamins B6, B9, and B12 can lead to increased levels of plasma homocysteine (Mudd et al., 1964; Selhub et al., 1993; Rozen, 1997; Lentz et al., 2000; Chen et al., 2001), termed hyperhomocysteinemia (HHcy). HHcy is a risk factor for both vascular cognitive impairment and dementia (VCID) and Alzheimer's disease (AD; Bostom et al., 1999; Eikelboom et al., 1999; Van Dam and Van Gool, 2009). Previous studies have shown that serum homocysteine levels are inversely related to cognitive function in patients with dementia and elevated levels are more common in VCID patients than AD patients (Miller et al., 2002; Clarke et al., 2003). While studies have shown an association between homocysteine levels and hippocampal atrophy, white matter lesions, and lacunar infarcts, the mechanism of homocysteine-induced

[1]Sanders-Brown Center on Aging, University of Kentucky, Lexington, KY, USA
[2]Department of Physiology, University of Kentucky, Lexington, KY, USA
[*]These authors contributed equally to this work.

Corresponding Author:
Donna M. Wilcock, University of Kentucky, Room 101B, 800 S Limestone St, Lexington, KY 40536, USA.
Email: donna.wilcock@uky.edu

damage remains unknown (Vermeer et al., 2002; Firbank et al., 2010).

Our group has been working on HHcy induction in mice as a model of VCID. In both mouse and humans, 5 to 12 μM of homocysteine is considered normal, 12 to 30 μM is categorized as mild HHcy, 30 to 100 μM is moderate HHcy, and anything above 100 μM is considered severe HHcy. In C57BL/6 mice, dietary HHcy induction through deficiency in vitamins B6, B9, and B12 and enrichment in methionine results in homocysteine levels between 50 and 80 μM, thus inducing moderate HHcy (Sudduth et al., 2013). Microhemorrhages were the main cerebrovascular pathology noted in the HHcy mice and behavior testing showed significant cognitive deficits in these mice. Moderate HHcy also induced a proinflammatory phenotype, reduced cerebral blood flow, and increased activity of matrix metalloproteinase 2 (MMP2) and MMP9, which are known to degrade tight junctions in the blood–brain barrier (Klein and Bischoff, 2011).

Dietary induction of HHcy in amyloid precursor protein (APP)/PS1 mice produces a comorbidity mouse model with aspects of both AD and VCID (Sudduth et al., 2014). During the radial arm water maze, the comorbidity mouse model displayed additive cognitive deficits. Clinically, it has been shown that comorbidity patients show an additive effect on test scores for memory and executive function, thus making this a clinically relevant model (Reed et al., 2007). Induction of HHcy in APP/PS1 mice produced a switch from an anti-inflammatory phenotype to a proinflammatory phenotype and significantly increased MMP9 and MMP2 activity. While there were not significant changes in total Aβ levels, we did see a change in the location of Aβ, with more accumulating around the vasculature. Finally, these comorbidity mice had a significant increase in microhemorrhages.

It remains unclear from our *in vivo* studies what the effects of homocysteine are on the individual cell types of the brain, which could help us elucidate possible therapeutic targets. To determine the cell specific effects of HHcy, we took separate cultures of C8-D1A astrocytes, BV2 microglia cells, primary endothelial cells, and N2a neuronal cells and treated them with 50 μM of homocysteine for 24, 48, 72, and 96 hr. For each cell type, we analyzed the gene expression of several cell type specific markers, inflammatory markers, and MMP9 system markers.

Materials and Methods

C8-D1A Cell Culture

C8-D1A cells were obtained directly from American Type Culture Collection (Catalogue No. CRL-2541, Manassas, VA). Cells were grown in 75 cm^2 flasks in DME media containing 10% fetal bovine serum and 1% penicillin-streptomycin (Life Technologies, Carlsbad, CA) until approximately 80% confluency was reached, usually after 7 days.

BV2 Cell Culture

BV2 cells, originally developed by Elisabetta Blasi et al. (1990; courtesy of Dr. Linda Van Eldik), were grown in petri dishes in DME media with nutrient mixture F12 containing 10% fetal bovine serum, 1% serum L-glutamate, and 1% penicillin-streptomycin (Life Technologies, Carlsbad, CA) until approximately 80% confluency was reached, usually after 3 days.

Primary Endothelial Cell Culture

C57BL/6 mouse primary brain microvascular endothelial cells were obtained directly from Cell Biologics (Catalogue No. C57-6023, Chicago, IL). Cells were grown in 75 cm^2 flasks coated with a gelatin-based coating solution (Cell Biologics, Chicago, IL). Endothelial cell media containing vascular endothelial growth factor, endothelial cell growth supplement, heparin, epidermal growth factor, hydrocortisone, L-glutamine, an antibiotic-antimycotic solution, and fetal bovine serum (Complete Mouse Endothelial Cell Medium w/ Kit, Cell Biologics, Chicago, IL) was used to grow the endothelial cells to approximately 80% confluency.

N2a Cell Culture

N2a cells (courtesy of Dr. John Gensel; Olmsted et al., 1971) were grown in 75 cm^2 flasks in Opti-MEM media containing 40% DME media, 10% fetal bovine serum, and 1% penicillin-streptomycin (Life Technologies, Carlsbad, CA) until approximately 80% confluency was reached, usually after 3 days.

HHcy Treatment

Once the cells reached 80% confluency, the cells were trypsinized and resuspended in 10 mL of media with serum. For the BV2 and N2a cells, 100 μL of cells were placed in each well of a six-well plate. For the C8-D1A cells, 500 μL of cells were placed in each well of a six-well plate. For the endothelial cells, 1 mL of cells were placed in a 25 cm^2 flask coated with a gelatin-based coating solution (Cell Biologics, Chicago, IL). For all cells, the volume in each well or flask was brought up to 2 mL with media containing serum.

Once the cells reached 60% to 70% confluency, media with serum was replaced with serum-free media for 24 hr to avoid unwanted stimulation by serum components. To determine the optimal dose of HHcy, BV2 cells were treated with either 5 μM, 15 μM, 50 μM, or 100 μM of homocysteine (Sigma, St. Louis, MO) for 24 hr. Based

on the results in Figure 1(a), 50 μM was used to treat all cell types since each cell would be exposed to the same levels *in vivo*.

After 24 hr in serum-free media, each cell type was treated with either 50 μM homocysteine or remained in serum-free media as a control for 24, 48, 72, or 96 hr. Media was changed every 2 days. Media was aspirated and cells were rinsed in 1X DPBS (Life Technologies, Carlsbad, CA) and frozen at −20° until RNA isolation. Cell treatments were run at least twice for each cell line in groups of two or three ($N = 4$ to 6 per group).

Cell viability was determined at 48 and 96 hr for each cell type. The media from each well or flask was combined with the trypsinized cells and resuspended in 2 mL of media. After 500 μL of the resuspended cells was combined with 500 μL of trypan blue (Amresco, Solon, OH), 10 μL of this mixture was loaded on a hemocytometer. The number of dead and live cells were counted from four grids and averaged.

All cells were incubated at 5% CO_2 at 37°C.

Quantitative Reverse Transcription Polymerase Chain Reaction

Total mRNA was extracted from the frozen cells using cells scrapers in lysis buffer from the RNeasy Mini-kit (Qiagen, Valencia, CA). The subsequent steps of the extraction were done according to the manufacturer's

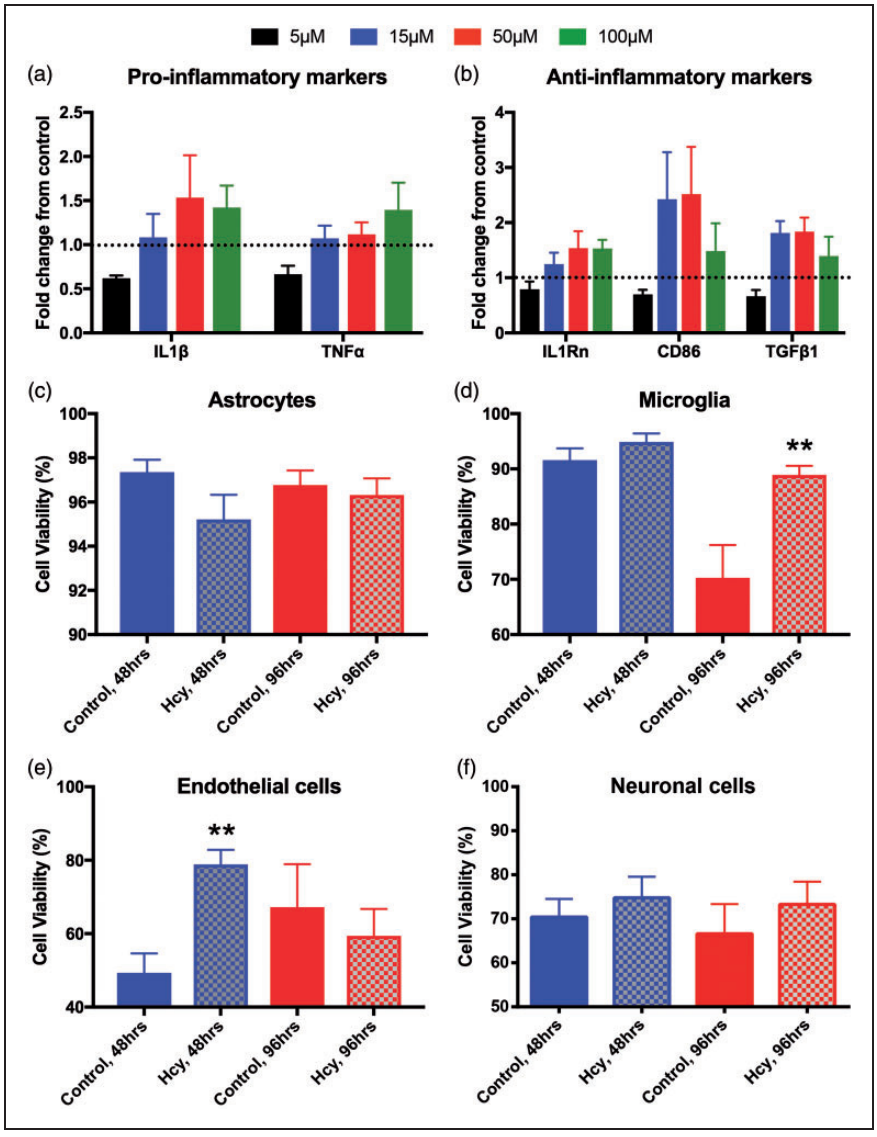

Figure 1. Homocysteine dose response and cell viability. Relative gene expression of (a) proinflammatory and (b) anti-inflammatory markers in BV2 microglial cells after 24 hr of treatment with homocysteine. Data are shown as a fold change from control-treated cells. Cell viability of (c) astrocytes, (d) microglia, (e) endothelial cells, and (f) neuronal cells after treatment with 50 μM of homocysteine for 48 and 96 hr. ** indicates a p value $< .01$ compared with control-treated cells for that time point.

instructions. The Biospec-Nano Spectrophotometer (Shimadzu, Kyoto, Japan) was used to quantify the nucleic acid concentration of each sample. cDNA was transcribed using the High Capacity kit (ThermoFisher, Walthan, MA) according to the manufacturer's instructions. The cDNA was produced using the Veriti^{TM} 96-well Thermocycler (Applied Biosystems, Grand Island, NY) through heating and annealing cycles.

Quantitative Reverse Transcription Polymerase Chain Reaction (RT-PCR) was performed using the Fast-TaqMan Gene Expression kit (Life Technologies, Carlsbad, CA) in 96-well plates. In each well, 1 μL of the appropriate gene probe (Life Technologies, Carlsbad, CA) listed in Table 1 was added to 10 μL of the Fast-TaqMan reagent along with 0.5 μL of cDNA and 6.5 μL of RNAse-free water for a final volume of 18 μL. Real-time RT-PCR was performed using the ViiA^{TM}7 Real-Time PCR system (Applied Biosystems, Grand Island, NY). All genes were normalized to the 18 S rRNA gene. Fold change was determined using the $-\Delta\Delta$Ct method and the homocysteine treated cells were compared with the control cells of the appropriate time point.

Analysis

Data are presented as mean ± SEM. Statistical analysis was performed using the JMP statistical analysis software program (SAS Institute, Cary, NC). Student's *t*-test were performed and statistical significance was assigned when the *p*-value was $< .05$.

Table 1. Genes for Real-Time PCR.

Gene of interest	PMID	Taqman ID
IL1β	NM_008361.3	Mm.222830
TNFα	NM_013693.3	Mm.1293
IL1Ra	NM_031167.5	Mm.882
CD86	NM_019388.3	Mm.1452
TGFβ1	NM_011577.1	Mm.248380
MRC1	NM_008625.2	Mm.2019
MMP3	NM_010809.1	Mm.4993
MMP9	NM_013599.3	Mm.4406
TIMP1	NM_001044384.1	Mm.8245
AQP4	NM_009700.2	Mm.250786
GFAP	NM_001131020.1	Mm.1239
KCNJ10	NM_001039484.1	Mm.254563
KCNMA1	NM_001253358.1	Mm.343607
PECAM1	AK037551.1	Mm.343951
CLDN5	NM_013805.4	Mm.22768
OCEL1	NM_008756.2	Mm.4807
COL4α5	NM_001163155.1	Mm.286892
APP	NM_001198823.1	Mm.277585
GRN	NM_008175.4	Mm.1568
GSK3β	NM_019827.6	Mm.394930
PPP2CA	NM_019411.4	Mm.00479816

Results

To determine the dose response to homocysteine, BV2 cells were treated with 5, 15, 50, or 100 μM of homocysteine for 24 hr (Figure 1(a) and (b)). Treatment of BV2 cells with 50 μM of homocysteine, which is considered moderate HHcy, resulted in the highest gene expression levels of several pro- and anti-inflammatory markers, specifically interleukin 1 beta (IL1β), interleukin 1 receptor antagonist (IL1Ra), cluster of differentiation 86 (CD86), and transforming growth factor beta 1 (TGFβ1); therefore, 50 μM was used uniformly across all cell types. Importantly, in our mice, we achieve 50 to 80 μM levels of homocysteine in plasma (Sudduth et al., 2013; Weekman et al., 2016). Cell viability for each cell type was also determined after exposure to homocysteine for 48 or 96 hr. Astrocytes had a slight decrease in cell viability only at 48 hr, but this was not significant (Figure 1(c)). At 48 hr, there was a slight increase in microglia cell viability when exposed to homocysteine, and this became significant by 96 hr (Figure 1(d)). Endothelial cells had a significant increase in cell viability at 48 hr but decreased at 96 hr (Figure 1(e)). At both 48 and 96 hr, neuronal cells had slight increases in cell viability after treatment with homocysteine; however, this was not significant (Figure 1(f)). Most importantly, no significant cell death was observed with homocysteine treatment in any of the cell types studied.

We also determined changes in the gene expression of several pro- and anti-inflammatory markers when astrocytes, microglia, endothelial cells, and neuronal cells were exposed to homocysteine. Astrocytes show no significant changes in the proinflammatory marker tumor necrosis factor alpha (TNFα; Figure 2(a)). However, there was a significant decrease in the anti-inflammatory marker IL1Ra at 48 hr when compared with controls. There was also an overall trend for decreased IL1Ra up to 72 hr, but levels increased again at 96 hr. The other anti-inflammatory marker, TGFβ1, was slightly increased at 48 hr but decreased at 72 hr.

Microglia cells treated with homocysteine had a significant increase in the proinflammatory marker IL1β and a slight but nonsignificant increase in TNFα at 48 hr (Figure 2(c)). There was also a significant increase in the anti-inflammatory marker TGFβ1 at 48 hr. Levels of IL1β, TNFα, and TGFβ1 were decreased at 72 hr and again at 96 hr when compared with 48 hr homocysteine-treated cells (Figure 2(c) and (d)). At 72 hr, IL1Ra levels were significantly increased when compared with controls and when compared with 48 hr

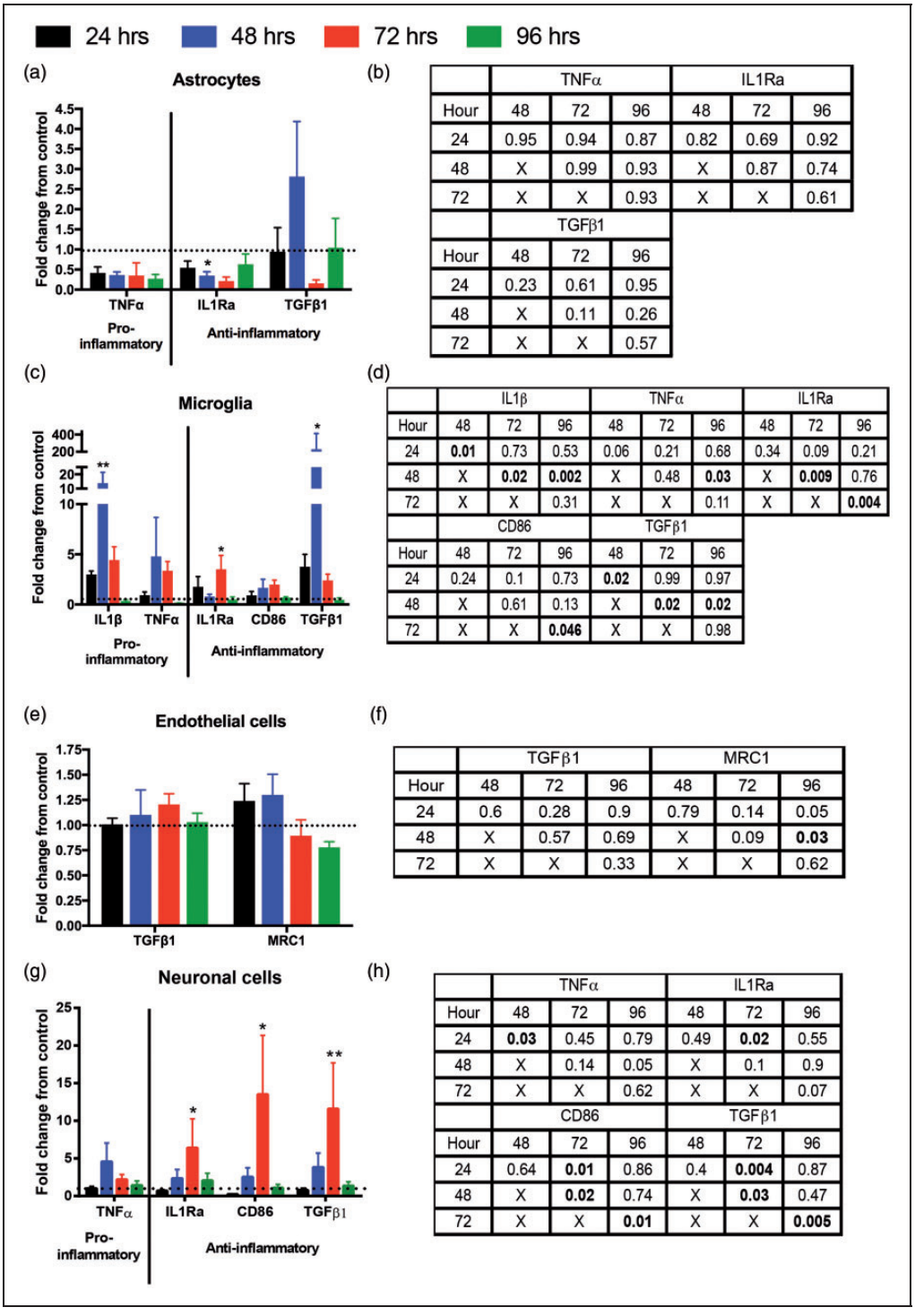

(b)

	TNFα			IL1Ra		
Hour	48	72	96	48	72	96
24	0.95	0.94	0.87	0.82	0.69	0.92
48	X	0.99	0.93	X	0.87	0.74
72	X	X	0.93	X	X	0.61
	TGFβ1					
Hour	48	72	96			
24	0.23	0.61	0.95			
48	X	0.11	0.26			
72	X	X	0.57			

(d)

	IL1β			TNFα			IL1Ra		
Hour	48	72	96	48	72	96	48	72	96
24	**0.01**	0.73	0.53	0.06	0.21	0.68	0.34	0.09	0.21
48	X	**0.02**	**0.002**	X	0.48	**0.03**	X	**0.009**	0.76
72	X	X	0.31	X	X	0.11	X	X	**0.004**
	CD86			TGFβ1					
Hour	48	72	96	48	72	96			
24	0.24	0.1	0.73	**0.02**	0.99	0.97			
48	X	0.61	0.13	X	**0.02**	**0.02**			
72	X	X	**0.046**	X	X	0.98			

(f)

	TGFβ1			MRC1		
Hour	48	72	96	48	72	96
24	0.6	0.28	0.9	0.79	0.14	0.05
48	X	0.57	0.69	X	0.09	**0.03**
72	X	X	0.33	X	X	0.62

(h)

	TNFα			IL1Ra		
Hour	48	72	96	48	72	96
24	**0.03**	0.45	0.79	0.49	**0.02**	0.55
48	X	0.14	0.05	X	0.1	0.9
72	X	X	0.62	X	X	0.07
	CD86			TGFβ1		
Hour	48	72	96	48	72	96
24	0.64	**0.01**	0.86	0.4	**0.004**	0.87
48	X	**0.02**	0.74	X	**0.03**	0.47
72	X	X	**0.01**	X	X	**0.005**

Figure 2. Neuroinflammation markers. Relative gene expression changes for pro- and anti-inflammatory markers in (a) astrocytes, (c) microglia, (e) endothelial cells, and (g) neuronal cells. Data are shown as a fold change from control-treated cells for that time point. *indicates a p value $< .05$ and ** indicates a p value $< .01$ compared with control-treated cells for that time point. p values for homocysteine-treated comparisons for (b) astrocytes, (d) microglia, (f) endothelial cells, and (h) neuronal cells. Significant differences are shown in bold.

homocysteine-treated cells. Levels of IL1Ra were significantly decreased by 96 hr when compared with 72 hr homocysteine-treated cells. The other anti-inflammatory marker, CD86, had slight increases up to 72 hr and a decrease at 96 hr that was significantly different from the 72 hr homocysteine-treated cells.

Endothelial cells only had a significant decrease in the anti-inflammatory marker mannose receptor C Type 1 at

96 hr when compared with 48 hr homocysteine-treated cells (Figure 2(e) and (f)).

Neuronal cells treated with homocysteine had a slight increase in TNFα at 48 hr but was only significant when compared with 24 hr homocysteine-treated cells (Figure 2(g) and (h)). The anti-inflammatory markers (IL1Ra, CD86, and TGFβ1) showed increased levels with a significant peak at 72 hr when compared with controls. CD86 and TGFβ1 were significantly decreased at 96 hr when compared with 72 hr homocysteine-treated cells. It should be noted that while the fold changes for these inflammatory markers are dramatic, the qPCR cycle numbers were high, indicating the expression level was extremely low in these neuronal cells.

The MMP9 system has been implicated in the tight junction breakdown leading to microhemorrhages in AD and VCID; therefore, we assessed the changes in the gene expression levels of the MMP9 system markers in response to homocysteine. In astrocytes, there was a slight increase in MMP3 expression over 96 hr, but this was not significant (Figure 3(a)). However, MMP9 expression was significantly increased at 48 hr when compared with controls. Levels of MMP9 were significantly decreased again at 72 and 96 hr when compared with the 48 hr treated homocysteine cells (Figure 3(b)). Tissue inhibitor of matrix metalloproteinase 1 (TIMP1) gene expression levels increased over time, with 96 hr being significantly increased when compared with controls and when compared with 24 and 48 hr homocysteine-treated cells.

Microglia had slightly increased MMP9 levels at 24 hr, but this was not significant (Figure 3(c)). Levels of MMP9 were significantly increased at 72 hr when compared with controls and when compared with 24, 48, and 96 hr homocysteine-treated cells (Figure 3(d)). TIMP1 levels were significantly increased at 96 hr when compared with controls and when compared with 48 and 72 hr homocysteine-treated cells.

Endothelial cells treated with homocysteine had significantly increased levels of MMP3 at 48 hr when compared with controls (Figure 3(e)). However, MMP9 levels, while slightly increased at 24 hr, were significantly decreased at 48 and 96 hr when compared with 24 hr homocysteine-treated cells (Figure 3(f)). Levels were returned to normal at 72 hr. TIMP1 was only slightly increased at 48 hr with no significant changes. Neuronal cells only had slight increases in both MMP9 and TIMP1 at 72 hr with levels returning to normal at 96 hr (Figure 3(g) and (h)).

Astrocytes treated with homocysteine show a trend for decreased aquaporin 4 (AQP4) levels up to 72 hr and then increase again at 96 hr; however, this was not significant when compared with controls (Figure 4(a)). Glial fibrillary acidic protein levels increased up to 72 hr and then decreased at 96 hr, but again this was not significant when compared with controls. The adenosine triphosphate (ATP)-sensitive inward rectifier potassium channel 10 (KCNJ10) had significantly increased gene expression levels at 24 hr when compared with controls. However, by 48 and 72 hr, levels were significantly decreased when compared with the 24 hr homocysteine-treated cells (Figure 4(b)). Levels of KCNJ10 were significantly increased at 96 hr when compared with 72 hr homocysteine-treated cells. Another potassium channel, potassium calcium-activated channel subfamily M alpha 1 (KCNMA1) was slightly decreased at 72 hr, but was not significant.

Endothelial cells treated with homocysteine showed no changes in platelet endothelial cell adhesion molecule 1 gene expression levels over the 96 hr (Figure 4(c)). Claudin-5 levels had increasing levels with a peak at 72 hr. Levels of claudin-5 were significantly decreased at 96 hr when compared with 72 hr homocysteine-treated cells (Figure 4(d)). Occludin levels were significantly decreased at 48 hr when compared with controls but levels were significantly higher at 72 hr when compared with 48 and 96 hr homocysteine-treated controls. Collagen Type IV alpha 5 had decreased levels with a peak at 72 hr. Levels were significantly increased at 96 hr when compared with 24, 48, and 72 hr homocysteine-treated cells.

Neuronal cells treated with homocysteine had slight increases in APP and granulin at 48 hr but levels decreased at 72 hr and further decreased at 96 hr (Figure 4(e)); however, none of these changes were significant. Both glycogen synthase kinase 3 beta (GSK3β), serine/threonine-protein phosphatase 2 A (PPP2CA), and KCNMA1 had increased gene expression levels up to 72 hr but decreased at 96 hr when compared with 72 hr homocysteine-treated cells (Figure 4(f)). KCNJ10 had significantly increased levels at 48 hr when compared with controls and levels were significantly decreased at 72 hr when compared with 48 hr homocysteine-treated cells.

Discussion

HHcy is a risk factor for both VCID and AD, the two most common forms of dementia. Our lab has developed a mouse model that induces HHcy to model VCID. In this mouse model, we see cognitive deficits, an increase in microglial staining, a proinflammatory phenotype, and a significant increase in microhemorrhages (Sudduth et al., 2013). While we know the overall effect of HHcy on the brain, there is limited information on the cell specific effects of HHcy. We took cell cultures of astrocytes, microglia, endothelial cells, and neuronal cells and treated them with homocysteine to determine gene expression changes specific to each cell type. Astrocytes showed a decrease in two potassium channels and aquaporin 4

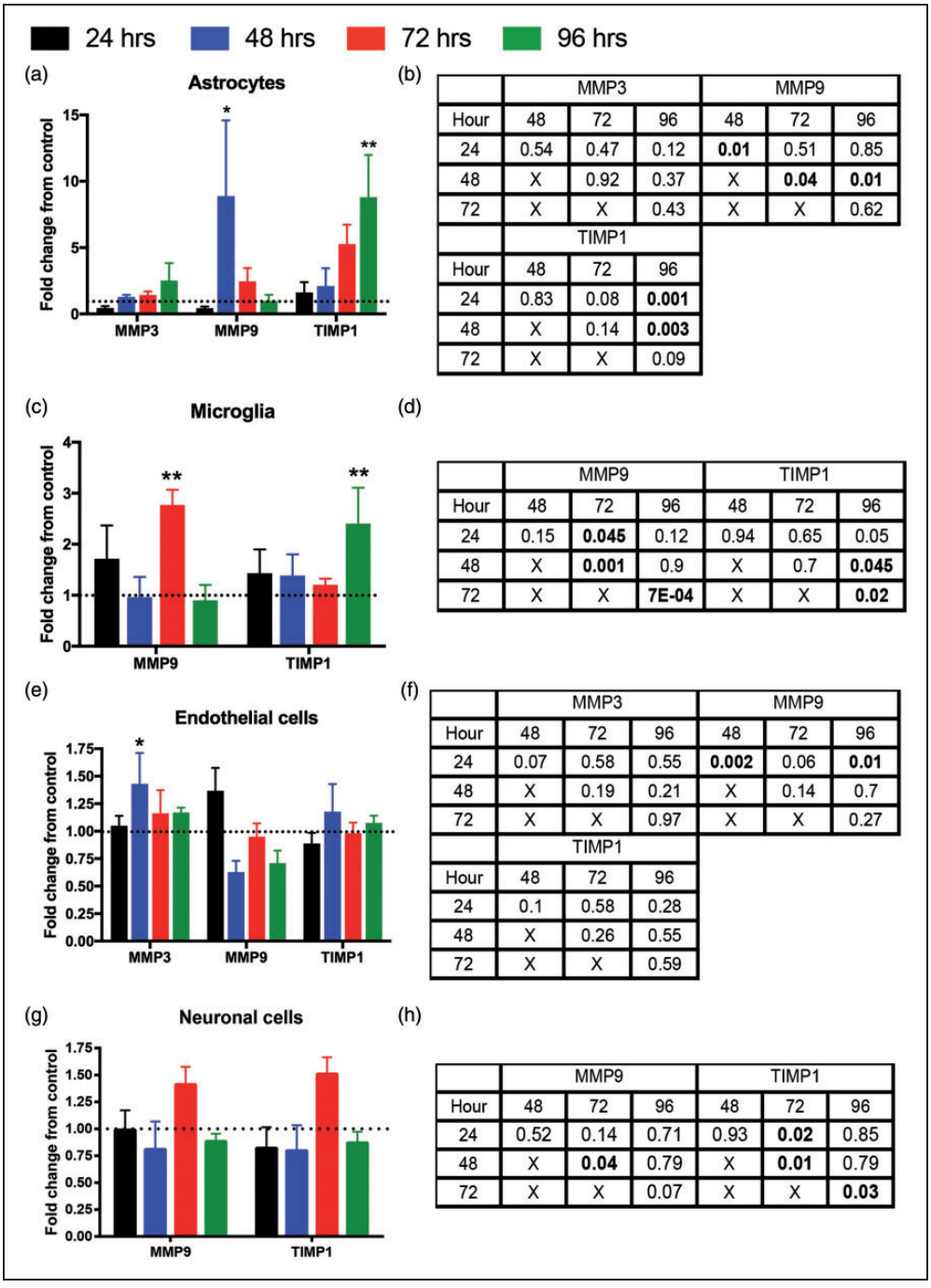

(b)

	MMP3			MMP9		
Hour	48	72	96	48	72	96
24	0.54	0.47	0.12	**0.01**	0.51	0.85
48	X	0.92	0.37	X	**0.04**	**0.01**
72	X	X	0.43	X	X	0.62

	TIMP1		
Hour	48	72	96
24	0.83	0.08	**0.001**
48	X	0.14	**0.003**
72	X	X	0.09

(d)

	MMP9			TIMP1		
Hour	48	72	96	48	72	96
24	0.15	**0.045**	0.12	0.94	0.65	0.05
48	X	**0.001**	0.9	X	0.7	**0.045**
72	X	X	**7E-04**	X	X	**0.02**

(f)

	MMP3			MMP9		
Hour	48	72	96	48	72	96
24	0.07	0.58	0.55	**0.002**	0.06	**0.01**
48	X	0.19	0.21	X	0.14	0.7
72	X	X	0.97	X	X	0.27

	TIMP1		
Hour	48	72	96
24	0.1	0.58	0.28
48	X	0.26	0.55
72	X	X	0.59

(h)

	MMP9			TIMP1		
Hour	48	72	96	48	72	96
24	0.52	0.14	0.71	0.93	**0.02**	0.85
48	X	**0.04**	0.79	X	**0.01**	0.79
72	X	X	0.07	X	X	**0.03**

Figure 3. MMP9 system markers. Relative gene expression changes for MMP9 system markers in (a) astrocytes, (c) microglia, (e) endothelial cells, and (g) neuronal cells. Data are shown as a fold change from control-treated cells for that time point. * indicates a p value $< .05$ and ** indicates a p value $< .01$ compared with control-treated cells for that time point. p values for homocysteine-treated comparisons for (b) astrocytes, (d) microglia, (f) endothelial cells, and (h) neuronal cells. Significant differences are shown in bold.

with lows at 72 hr. Microglia cells showed an initial increase in proinflammatory markers at 48 hr but then an increase in anti-inflammatory markers at 72 hr. Endothelial cells showed an increase in claudin-5 up to 72 hr but a decrease in occludin at 48 hr. Neurons treated with homocysteine showed an increase in two potassium channels, GSK3β and PPP2CA as well as increases in anti-inflammatory markers with peaks at 72 hr.

Inflammation has been implicated as a possible mechanism for vascular damage in VCID (Rosenberg, 2009) and induction of HHcy in mice to model VCID has shown a proinflammatory response (Sudduth et al.,

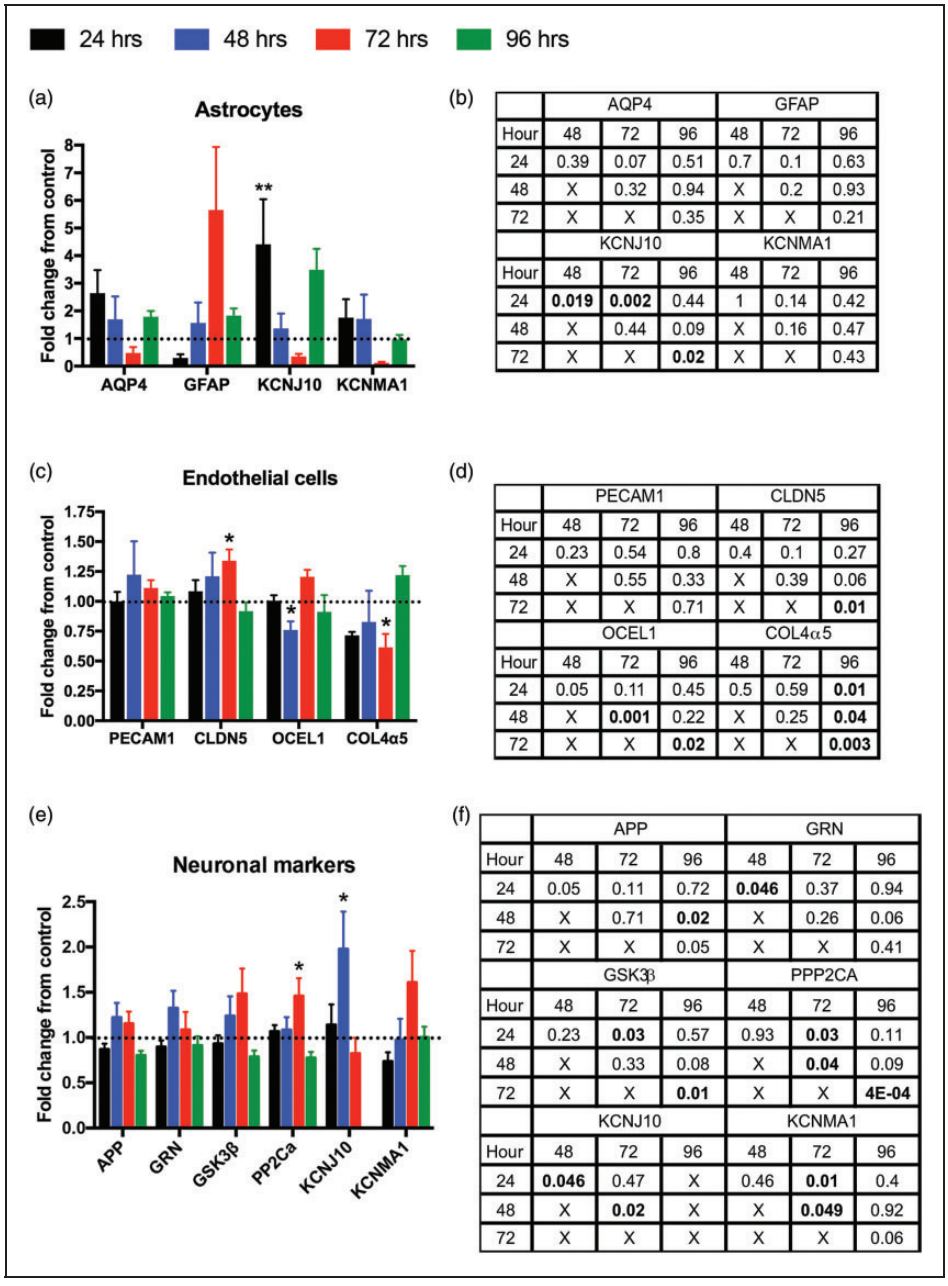

(b)

	AQP4			GFAP		
Hour	48	72	96	48	72	96
24	0.39	0.07	0.51	0.7	0.1	0.63
48	X	0.32	0.94	X	0.2	0.93
72	X	X	0.35	X	X	0.21
	KCNJ10			KCNMA1		
Hour	48	72	96	48	72	96
24	**0.019**	**0.002**	0.44	1	0.14	0.42
48	X	0.44	0.09	X	0.16	0.47
72	X	X	**0.02**	X	X	0.43

(d)

	PECAM1			CLDN5		
Hour	48	72	96	48	72	96
24	0.23	0.54	0.8	0.4	0.1	0.27
48	X	0.55	0.33	X	0.39	0.06
72	X	X	0.71	X	X	**0.01**
	OCEL1			COL4α5		
Hour	48	72	96	48	72	96
24	0.05	0.11	0.45	0.5	0.59	**0.01**
48	X	**0.001**	0.22	X	0.25	**0.04**
72	X	X	**0.02**	X	X	**0.003**

(f)

	APP			GRN		
Hour	48	72	96	48	72	96
24	0.05	0.11	0.72	**0.046**	0.37	0.94
48	X	0.71	**0.02**	X	0.26	0.06
72	X	X	0.05	X	X	0.41
	GSK3β			PPP2CA		
Hour	48	72	96	48	72	96
24	0.23	**0.03**	0.57	0.93	**0.03**	0.11
48	X	0.33	0.08	X	**0.04**	0.09
72	X	X	**0.01**	X	X	**4E-04**
	KCNJ10			KCNMA1		
Hour	48	72	96	48	72	96
24	**0.046**	0.47	X	0.46	**0.01**	0.4
48	X	**0.02**	X	X	**0.049**	0.92
72	X	X	X	X	X	0.06

Figure 4. Cell-specific markers. Relative gene expression changes for cell-specific markers in (a) astrocytes, (c) endothelial cells, and (e) neuronal cells. Data are shown as a fold change from control-treated cells for that time point. * indicates a p value $< .05$ and ** indicates a p value $< .01$ compared with control-treated cells for that time point. p values for homocysteine-treated comparisons for (b) astrocytes, (d) endothelial cells, and (f) neuronal cells. Significant differences are shown in bold.

2013), which can activate MMPs and lead to vascular breakdown and cognitive impairment. Inflammation has also been implicated in the disease process of AD and our comorbidity mice show a switch from an anti-inflammatory phenotype to a proinflammatory phenotype (Wyss-Coray et al., 2001; Herber et al., 2004; Kitazawa et al., 2005; Shaftel et al., 2007; Lee et al., 2010; Montgomery et al., 2011; Sudduth et al., 2012, 2014). Both microglia and astrocytes are capable of secreting inflammatory cytokines and proteases (Dong and Benveniste, 2001; Hanisch, 2002) in response to a variety of different stimuli, thus controlling the inflammatory phenotype. When treated with HHcy *in vitro*, microglia produce higher levels of several proinflammatory markers at 48 hr, which is similar to the proinflammatory response seen *in vivo* in our chronic HHcy mouse studies. By 72 hr, however, these levels of proinflammatory markers are reduced and there is an increase in an anti-inflammatory

marker. While our mouse models show a proinflammatory phenotype when on diet for 6 months, this cell data suggest that long-term exposure to HHcy would ultimately result in a switch to an anti-inflammatory phenotype. Astrocytes, neurons, and endothelial cells show a limited inflammatory response to HHcy with slight increases in anti-inflammatory markers around 48 and 72 hr. This shows that only microglia, rather than both microglia and astrocytes, are the inflammatory phenotype mediators when HHcy is present.

One of the major proteases involved in tight junction breakdown is MMP9 (Lee et al., 2003; Jickling et al., 2014), which can be activated via inflammation, specifically the proinflammatory cytokines TNFα and IL1β (Galis et al., 1994; Vecil et al., 2000). Our VCID mouse model shows a significant increase in activation of MMP9 as well as increases in TNFα and IL1β, providing a possible mechanism for the increase in microhemorrhages seen in the mouse model (Sudduth et al., 2013, 2014). Our *in vitro* data show that at 48 hr, astrocytes and endothelial cells are the major sources of MMP9 and MMP3, respectively. The increases seen in the MMP system, in particular MMP9, are parallel to those seen in the mouse model of HHcy. Treatment of individual cell types with homocysteine has provided insight into the major sources of MMP9 at different time points.

The response of cell specific genes to homocysteine can also generate therapeutic targets for treatment of VCID. In astrocytes, AQP4, KCNJ10, and KCNMA1 were decreased, similarly peaking at 72 hr. These potassium channels and AQP4 channel are associated with homeostatic control of potassium buffering, water balance, and are located at the astrocyte end-feet (Price et al., 2002; Simard and Nedergaard, 2004; Butt and Kalsi, 2006). We have shown a disruption in these channels and other astrocytic end-feet channels in our VCID mouse model (Sudduth et al., 2017). The fact that HHcy can directly influence the expression of these channels was surprising and could highlight unique cellular mechanisms underlying the *in vivo* astrocytic disruptions previously observed. The decreases seen in these astrocytic end-feet genes could lead to disruption of the neurovascular unit and blood flow to these damaged areas, contributing to the cognitive decline seen in our mouse model. Endothelial cells also play a major role in the neurovascular unit by maintaining the tight junctions that make up the blood–brain barrier. Interruption of these tight junctions and consequently the blood–brain barrier can lead to microhemorrhages that damage the surrounding brain tissue. Treatment of endothelial cells showed a significant decrease in occludin, a major tight junction protein, at 48 hr. Homocysteine also induced an increase in claudin-5 gene expression levels which could compensate for the lowered occludin levels. However, while the gene expression of claudin-5 is increased, it may not equate to increased protein levels or even localization of the protein to the tight junctions. These disruptions in tight junctions could provide another mechanism via which HHcy causes microhemorrhages and cognitive decline by directly affecting tight junction gene expression levels, as opposed to our previous hypothesis that this was mediated by MMP degradation of tight junctions. HHcy is also a risk factor for AD (Van Dam and Van Gool, 2009), which is characterized by amyloid plaques and tangles made of hyperphosphorylated tau (Braak and Braak, 1995). APP and granulin, which are associated with AD and frontotemporal dementia, respectively, are not altered in neuronal cells when exposed to homocysteine, suggesting an alternate mechanism in which HHcy increases the risk of AD. There are alterations in the tau kinase GSK3β as well as changes in the tau phosphatase PPP2CA in the neuronal cells exposed to homocysteine. While these increases may cancel each other out, the gene expression changes may not lead to equal changes in protein levels or even protein activity for each. Further studies would be required to determine these changes in protein levels or activity, and provide a possible link between HHcy and AD. We have not observed significant tau changes in the mouse model of HHcy, but these data indicate that a more careful examination of tau state may be required.

The responses of specific cell types to homocysteine provide a starting point for future studies that could identify a wide variety of targets for AD and VCID therapeutics. For example, targeting microglia to reduce the release of proinflammatory cytokines could help reduce MMP9 activation leading to a decrease in tight junction breakdown. Astrocytic end-feet present another possible target to help reduce neurovascular damage and cognitive decline. GSK3β or PPP2CA could also be targeted to help reduce the risk of developing tauopathies in HHcy patients. The gene changes seen here have the potential to be biomarkers for VCID as well, and when compared with gene changes seen in AD, possible biomarkers for patients with VCID and AD. Other future studies would include cell specific functional changes in response to HHcy and interactions between cell lines when homocysteine is present.

Summary

Whether through genetic mutation or low levels of several B vitamins, increasing the levels of homocysteine in the brain can lead to gene expression changes in the major cell types of the brain, which can contribute to vascular cognitive impairment.

Acknowledgments

The authors would like to thank Dr. John Gensel for providing the N2a cell line and Dr. Linda Van Eldik for providing the BV2 cell line for this study.

Author Contributions

E. M. W. and A. E. W. performed the data collection and analysis, interpreted the data, and prepared the manuscript. T. L. S. assisted in data collection. D. M. W. conceived of the studies, analyzed, and interpreted the data and edited the final manuscript. All authors have approved the final version of the manuscript.

Declaration of Conflicting Interests

The author(s) declared no potential conflicts of interest with respect to the research, authorship, and/or publication of this article.

Funding

The author(s) disclosed receipt of the following financial support for the research, authorship, and/or publication of this article: Research reported in this manuscript was funded by fellowship F31NS092202 (EMW) and grants 1RO1NS079637 and 1RO1NS097722 (DMW) from the National Institutes of Health. The content is solely the responsibility of the authors and does not necessarily represent the ocial views of the National Institutes of Health.

References

Blasi, E., Barluzzi, R., Bocchini, V., Mazzolla, R., & Bistoni, F. (1990). Immortalization of murine microglial cells by a v-raf/v-myc carrying retrovirus. *J Neuroimmunol*, *27*, 229–237.

Bostom, A. G., Rosenberg, I. H., Silbershatz, H., Jacques, P. F., Selhub, J., D'Agostino, R. B., Wilson, P. W., . . . Wolf, P. A. (1999). Nonfasting plasma total homocysteine levels and stroke incidence in elderly persons: The Framingham Study. *Ann Intern Med*, *131*, 352–355.

Braak, H., & Braak, E. (1995). Staging of Alzheimer's disease-related neurofibrillary changes. *Neurobiol Aging*, *16*, 271–278; discussion 278–284.

Butt, A. M., & Kalsi, A. (2006). Inwardly rectifying potassium channels (Kir) in central nervous system glia: A special role for Kir4.1 in glial functions. *J Cell Mol Med*, *10*, 33–44.

Chen, Z., Karaplis, A. C., Ackerman, S. L., Pogribny, I. P., Melnyk, S., Lussier-Cacan, S., Chen, M. F., Pai, A., John, S. W., Smith, R. S., Bottiglieri, T., Bagley, P., Selhub, J., Rudnicki, M. A., James, S. J., & Rozen, R. (2001). Mice deficient in methylenetetrahydrofolate reductase exhibit hyperhomocysteinemia and decreased methylation capacity, with neuropathology and aortic lipid deposition. *Hum Mol Genet*, *10*, 433–443.

Clarke, R., Harrison, G., Richards, S, & Vital Trial Collaborative Group. (2003). Effect of vitamins and aspirin on markers of platelet activation, oxidative stress and homocysteine in people at high risk of dementia. *J Intern Med*, *254*, 67–75.

Dong, Y., & Benveniste, E. N. (2001). Immune function of astrocytes. *Glia*, *36*, 180–190.

Eikelboom, J. W., Lonn, E., Genest, J. Jr., Hankey, G., & Yusuf, S. (1999). Homocyst(e)ine and cardiovascular disease: A critical review of the epidemiologic evidence. *Ann Intern Med*, *131*, 363–375.

Firbank, M. J., Narayan, S. K., Saxby, B. K., Ford, G. A., & O'Brien, J. T. (2010). Homocysteine is associated with hippocampal and white matter atrophy in older subjects with mild hypertension. *Int Psychogeriatr*, *22*, 804–811.

Galis, Z. S., Muszynski, M., Sukhova, G. K., Simon-Morrissey, E., Unemori, E. N., Lark, M. W., Amento, E., & Libby, P. (1994). Cytokine-stimulated human vascular smooth muscle cells synthesize a complement of enzymes required for extracellular matrix digestion. *Circ Res*, *75*, 181–189.

Hanisch, U. K. (2002). Microglia as a source and target of cytokines. *Glia*, *40*, 140–155.

Herber, D. L., Roth, L. M., Wilson, D., Wilson, N., Mason, J. E., Morgan, D., & Gordon, M. N. (2004). Time-dependent reduction in Abeta levels after intracranial LPS administration in APP transgenic mice. *Exp Neurol*, *190*, 245–253.

Jickling, G. C., Liu, D., Stamova, B., Ander, B. P., Zhan, X., Lu, A., & Sharp, F. R. (2014). Hemorrhagic transformation after ischemic stroke in animals and humans. *J Cerebr Blood Flow Metabol*, *34*, 185–199.

Kitazawa, M., Oddo, S., Yamasaki, T. R., Green, K. N., & LaFerla, F. M. (2005). Lipopolysaccharide-induced inflammation exacerbates tau pathology by a cyclin-dependent kinase 5-mediated pathway in a transgenic model of Alzheimer's disease. *J Neurosci*, *25*, 8843–8853.

Klein, T., & Bischoff, R. (2011). Physiology and pathophysiology of matrix metalloproteases. *Amino Acids*, *41*, 271–290.

Lee, D. C., Rizer, J., Selenica, M. L., Reid, P., Kraft, C., Johnson, A., Blair, L., Gordon, M. N., Dickey, C. A., . . . Morgan, D. (2010). LPS-induced inflammation exacerbates phospho-tau pathology in rTg4510 mice. *J Neuroinflammation*, *7*, 56.

Lee, J. M., Yin, K. J., Hsin, I., Chen, S., Fryer, J. D., Holtzman, D. M., Hsu, C. Y., & Xu, J. (2003). Matrix metalloproteinase-9 and spontaneous hemorrhage in an animal model of cerebral amyloid angiopathy. *Ann Neurol*, *54*, 379–382.

Lentz, S. R., Erger, R. A., Dayal, S., Maeda, N., Malinow, M. R., Heistad, D. D., & Faraci, F. M. (2000). Folate dependence of hyperhomocysteinemia and vascular dysfunction in cystathionine beta-synthase-deficient mice. *Am J Physiol Heart Circ Physiol*, *279*, H970–H975.

Miller, J. W., Green, R., Mungas, D. M., Reed, B. R., & Jagust, W. J. (2002). Homocysteine, vitamin B6, and vascular disease in AD patients. *Neurology*, *58*, 1471–1475.

Montgomery, S. L., Mastrangelo, M. A., Habib, D., Narrow, W. C., Knowlden, S. A., Wright, T. W., & Bowers, W. J. (2011). Ablation of TNF-RI/RII expression in Alzheimer's disease mice leads to an unexpected enhancement of pathology: Implications for chronic pan-TNF-alpha suppressive therapeutic strategies in the brain. *Am J Pathol*, *179*, 2053–2070.

Mudd, S. H., Finkelstein, J. D., Irreverre, F., & Laster, L. (1964). Homocystinuria: An Enzymatic Defect. *Science*, *143*, 1443–1445.

Olmsted, J. B., Witman, G. B., Carlson, K., & Rosenbaum, J. L. (1971). Comparison of the microtubule proteins of neuroblastoma cells, brain, and Chlamydomonas flagella. *Proc Natl Acad Sci USA*, *68*, 2273–2277.

Price, D. L., Ludwig, J. W., Mi, H., Schwarz, T. L., & Ellisman, M. H. (2002). Distribution of rSlo Ca2+-activated K+ channels in rat astrocyte perivascular endfeet. *Brain Res*, *956*, 183–193.

Reed, B. R., Mungas, D. M., Kramer, J. H., Ellis, W., Vinters, H. V., Zarow, C., Jagust, W. J., & Chui, H. C. (2007). Profiles of neuropsychological impairment in autopsy-defined Alzheimer's disease and cerebrovascular disease. *Brain*, *130*, 731–739.

Rosenberg, G. A. (2009). Inflammation and white matter damage in vascular cognitive impairment. *Stroke*, *40*, S20–S23.

Rozen, R. (1997). Genetic predisposition to hyperhomocysteinemia: Deficiency of methylenetetrahydrofolate reductase (MTHFR). *Thromb Haemost*, *78*, 523–526.

Selhub, J., Jacques, P. F., Wilson, P. W., Rush, D., & Rosenberg, I. H. (1993). Vitamin status and intake as primary determinants of homocysteinemia in an elderly population. *JAMA*, *270*, 2693–2698.

Shaftel, S. S., Kyrkanides, S., Olschowka, J. A., Miller, J. N., Johnson, R. E., & O'Banion, M. K. (2007). Sustained hippocampal IL-1 beta overexpression mediates chronic neuroinflammation and ameliorates Alzheimer plaque pathology. *J Clin Investig*, *117*, 1595–1604.

Simard, M., & Nedergaard, M. (2004). The neurobiology of glia in the context of water and ion homeostasis. *Neuroscience*, *129*, 877–896.

Sudduth, T. L., Wilson, J. G., Everhart, A., Colton, C. A., & Wilcock, D. M. (2012). Lithium treatment of APPSwDI/NOS2-/- mice leads to reduced hyperphosphorylated tau, increased amyloid deposition and altered inflammatory phenotype. *PLoS One*, *7*, e31993.

Sudduth, T. L., Powell, D. K., Smith, C. D., Greenstein, A., & Wilcock, D. M. (2013). Induction of hyperhomocysteinemia models vascular dementia by induction of cerebral microhemorrhages and neuroinflammation. *J Cerebr Blood Flow Metabol*, *33*, 708–715.

Sudduth, T. L., Weekman, E. M., Brothers, H. M., Braun, K., & Wilcock, D. M. (2014). Beta-amyloid deposition is shifted to the vasculature and memory impairment is exacerbated when hyperhomocysteinemia is induced in APP/PS1 transgenic mice. *Alzheimers Res Ther*, *6*, 32.

Sudduth, T. L., Weekman, E. M., Price, B. R., Gooch, J. L., Woolums, A., Norris, C. M., & Wilcock, D. M. (2017). Time-course of glial changes in the hyperhomocysteinemia model of vascular cognitive impairment and dementia (VCID). *Neuroscience*, *341*, 42–51.

Van Dam, F., & Van Gool, W. A. (2009). Hyperhomocysteinemia and Alzheimer's disease: A systematic review. *Arch Gerontol Geriatr*, *48*, 425–430.

Vecil, G. G., Larsen, P. H., Corley, S. M., Herx, L. M., Besson, A., Goodyer, C. G., & Yong, V. W. (2000). Interleukin-1 is a key regulator of matrix metalloproteinase-9 expression in human neurons in culture and following mouse brain trauma *in vivo*. *J Neurosci Res*, *61*, 212–224.

Vermeer, S. E., van Dijk, E. J., Koudstaal, P. J., Oudkerk, M., Hofman, A., Clarke, R., & Breteler, M. M. (2002). Homocysteine, silent brain infarcts, and white matter lesions: The Rotterdam Scan Study. *Ann Neurol*, *51*, 285–289.

Weekman, E. M., Sudduth, T. L., Caverly, C. N., Kopper, T. J., Phillips, O. W., Powell, D. K., & Wilcock, D. M. (2016). Reduced efficacy of anti-abeta immunotherapy in a mouse model of amyloid deposition and vascular cognitive impairment comorbidity. *J Neurosci*, *36*, 9896–9907.

Wyss-Coray, T., Lin, C., Yan, F., Yu, G. Q., Rohde, M., McConlogue, L., Masliah, E., & Mucke, L. (2001). TGF-beta1 promotes microglial amyloid-beta clearance and reduces plaque burden in transgenic mice. *Nat Med*, *7*, 612–618.